Thesis for Master Degree

A Study on Top Heat Loss of a Closed Loop Oscillating Heat Pipes Solar Collector

Supervisor: Prof. Soek-Hun Yoon

February 2010

Graduate School of Korea Maritime University

Department of Marine System Engineering

Nguyen Kim Bao

A Study on Top Heat Loss of a Closed Loop Oscillating Heat Pipes Solar Collector

A Thesis By

Nguyen Kim Bao

Approved as to style and content by

Chairman	Prof. Tae-Woo Lim	(Sign)
Member	Prof. Jae-Hyuk Choi	(Sign)
Member	Prof. Soek-Hun Yoon	(Sign)

December 2009

Graduate School of Korea Maritime University

Department of Marine System Engineering

Acknowledgements

First of all, I would especially like to thank my supervisor, Professor Seok-Hun Yoon, who have been taught, helped, encouraged and supported me during last two years. I also would like to thank some professors who taught me at KMU including Professor You Teak Kim, Nam Chung Do, Jae Sung Choi, Cheol Oh.

I would like to thank to Professor Yun Chul Jung in Navigation Department, and my Rector, Professor Dang Van Uy, my Dean, Professor Nguyen Dai An and my senior, Dr. Nguyen Phung Hung in Vimaru who recommended me to my professor.

Thanks all my Vietnamese seniors, juniors, friends at Korea Maritime University including Dr. L. N. Q Lam, Mr. D. N. Hien, Dr. T. N. H. Son, Dr. N. D. Anh, Mr. N. T. Hoan, Mr. N. B. H. Anh, Mr. T. T. Do, Mr. T. X. Thuong and others at Ulsan Univ., Busan National Univ., and A Chu Univ.

Thanks all my Korean friends including Miss. Lee Mi Eun, Mr. Shin Woo Jung, Mr. Park Chi Byeong, Mr. Im Dae Won, and others.

Finally, I would like to express my deep gratitude to my parents, my sisters, my brothers and all my friends in Vietnam for their love, patience.

Korea Maritime University

December, 2009

Nguyen Kim Bao

A Study on Top Heat Loss of a Closed Loop Oscillating Heat Pipes Solar Collector

Nguyen Kim Bao

Graduate school of Korea Maritime University

Department of Marine system engineering

Abstract

In this study, a closed-loop oscillating heat pipes solar collector was constructed to investigate experimentally the effect of filling ratio of working fluid, flow rate of cooling water, and air gap thickness between absorber plate and glass cover on top heat loss and performance of the collector.

To absorb and transport thermal heat energy from heating to cooling section, closed-loop oscillating heat pipes was used combining with absorber plate/black chrome coating copper plate. The absorber plate was shined by solar simulator simulated by 12-300W halogen lamps. Top heat loss of the collector was determined basing on temperatures of absorber plate, glass cover, and ambient air that were measured and recorded by MV2000-Yokogawa recorder via K-type thermocouples.

Top heat loss of the collector were determined at the air gap thicknesses of 5mm, 15mm, 25mm and 35mm. Solar irradiation intensity was adjusted to 200W/m^2, 400W/m^2, 500W/m^2, 600W/m^2, 700W/m^2 and 800W/m^2. The results

show that the optimal air gap thickness for minimum top heat loss of the collector is 15mm.

Working fluid for the heat pipes was tested at filling ratios of 30% to 80%. Irradiation intensity was set to 545W/m^2, 645W/m^2, 718W/m^2 and 825W/m^2. The results show that top loss of the collector decreases dramatically at filling ratios of 60%, 70% at solar irradiation intensities of 545W/m^2, 645W/m^2, and 718w/m^2, 825w/m^2, respectively. The collector operates more effectively at filling ratio of 80% than that at 50%, 40%, and 30%.

Flow rate of cooling water was also investigated in this study. It was adjusted to 0.15l/min, 0.30l/min and 0.45l/min. The results show that flow rates of cooling water of 0.15l/min and 0.30l/min give the collector better performance than that of 0.45l/min.

Keywords: *Air gap thickness, closed-loop oscillating heat pipes (CLOHP), top loss coefficient, top heat loss, filling ratio (FR), cooling water flow rate (CWFR).*

Table of Contents

Acknowledgements iv

Abstract v

Nomenclatures ix

List of figures xi

Chapter 1 Introduction 1

Chapter 2 Theory analysis 4

2.1 Convective heat transfer coefficient 5

2.1.1 Heat transfer coefficient from absorber plate to cover (h_{1c}) 5

2.1.2 Heat transfer coefficient from cover to ambient air (h_{2c}) 6

2.2 Radiative heat transfer coefficient 6

2.2.1 From plate to cover (h_{1r}) 6

2.2.2 From cover to ambient (h_{2r}) 7

2.3 Top loss coefficient 7

Chapter 3 Collector design and experimental set-up 9

3.1 Collector design 9

3.2 Experimental set-up 10

Chapter 4 Results of experiment and discussion 14

4.1 Effect of the air gap thickness on thermal top heat loss 14

4.2 Effect of FR on top loss and thermal performance of the collector 21

4.3 Effect of flow rate of cooling water on the thermal performance of the collector 36

Chapter 5 Conclusions 39

References ……40

Nomenclatures

h_{1c} Convective heat transfer coefficient between plate and cover, [W/m^2 K]

Nu Nusselt number

Ra Rayleigh number

Gr Grashof number

Pr Prandtl number

g Acceleration of gravity, [m/s^2]

ΔT Temperature difference between plate and cover, [^{0}C]

Q_t Rate of top heat loss from front surface, [W]

L Air gap thickness between plate and cover, [m]

h_{2c} Convective heat loss coefficient from cover to ambient air, [W/m^2 K]

V Wind velocity, [m/s]

h_{1r} Radiative heat loss coefficient from plate to cover, [W/m^2 K]

T_P Absorber plate temperature, [^{0}C]

T_g Glass cover temperature, [^{0}C]

T_S Sky temperature, [^{0}C]

T_a Ambient air temperature, [^{0}C]

h_1 Total heat transfer coefficient from plate to cover, [W/m^2 K]

h_2 Total heat transfer coefficient from cover to ambient air, [W/m^2 K]

U_t Total top loss coefficient from plate to ambient, [W/m^2 K]

K Thermal conductivity of air, [W/m K]

A_c Area of collector, [m^2]

I Incident solar intensity, [W/m^2]

β Collector angle of inclination, [^{0}]

α Thermal diffusivity of air, [m^2/s]

ν Kinematic viscosity of air, [m^2/s]

σ Stefan's constant

ε_P Emissivity of absorber plate

ε_g Emissivity of glass cover

ε_{ff} Effective emissivity of plate-cover system

η Thermal efficiency [%]

q_u Useful energy [W]

m Flow rate of cooling water, [Kg/s]

C Specific heat of water [KJ/Kg.^{0}C]

ΔT_{cw} Difference of temperature of cooling water [^{0}C]

$$\beta' = \frac{1}{\frac{(T_P + T_g)}{2} + 273}$$

List of figures

Figure 2.1 Heat losses in a flat-plate solar collector 4

Figure 2.2 Thermal circuit diagram 8

Figure 3.1 Collector dimensions and configuration 9

Figure 3.2 Photo of the Collector 10

Figure 3.3 Schematic diagram of experimental set-up 11

Figure 3.4 Photo of the experimental set-up 12

Figure 4.1 Absorber plate temperature vs. air gap thickness 15

Figure 4.2 Glass cover temperature vs. air gap thickness 16

Figure 4.3 Plate - cover temperature difference vs. air gap thickness 16

Figure 4.4 Convective heat transfer coefficient vs. air gap thickness 17

Figure 4.5 Total top loss coefficient vs. air gap thickness 18

Figure 4.6 Rate of top heat loss vs. air gap thickness 18

Figure 4.7 Ratio of top loss to incident solar energy vs. air gap thickness 19

Figure 4.8 Absorber plate temperature vs. filling ratio 21

Figure 4.9 Glass cover temperature vs. filling ratio 21

Figure 4.10 T_1, T_2, P *vs. time at filling ratio of 30% and solar intensity of* $645W/m^2$ 23

Figure 4.11 T_1, T_2, P *vs. time at filling ratio of 40% and solar intensity of* $645W/m^2$ 23

Figure 4.12 T_1, T_2, P *vs. time at filling ratio of 50% and solar intensity of* $645W/m^2$ 24

Figure 4.13 T_1, T_2, P *vs. time at filling ratio of 60% and solar intensity of* $645W/m^2$ 24

Figure 4.14 T_1, T_2, P *vs. time at filling ratio of 70% and solar intensity of 645W/m²* 25

Figure 4.15 T_1, T_2, P *vs. time at filling ratio of 80% and solar intensity of 645 W/m²* 25

Figure 4.16 Total top loss coefficient vs. filling ratio.....26

Figure 4.17 T_1, T_2, P *vs. time at filling ratio of 60% and solar intensity of 545W/m²* 28

Figure 4.18 T_1, T_2, P *vs. time at filling ratio of 70% and solar intensity of 545W/m²* 28

Figure 4.19 T_1, T_2, P *vs. time at filling ratio of 80% and solar intensity of 545W/m²* 29

Figure 4.20 T_1, T_2, P *vs. time at filling ratio of 60% and solar intensity of 718W/m²* 29

Figure 4.21 T_1, T_2, P *vs. time at filling ratio of 70% and solar intensity of 718W/m²* 30

Figure 4.22 T_1, T_2, P *vs. time at filling ratio of 80% and solar intensity of 718W/m²* 30

Figure 4.23 T_1, T_2, P *vs. time at filling ratio of 60% and solar intensity of 825W/m²* 31

Figure 4.24 T_1, T_2, P *vs. time at filling ratio of 70% and solar intensity of 825W/m²* 31

Figure 4.25 T_1, T_2, P *vs. time at filling ratio of 80% and solar intensity of 825W/m²* 32

Figure 4.26 Rate of top heat loss vs. filling ratio 33

Figure 4.27 Ratio of top loss to incident solar energy vs. filling ratio.....33

Figure 4.28 Thermal efficiency vs. filling ratio at different solar intensity.....35

Figure 4.29 Thermal efficiency at different CWFR and solar intensity of 545W/m^2.....36

Figure 4.30 Thermal efficiency at different CWFR and solar intensity of 645W/m^2.....37

Figure 4.31 Thermal efficiency at different CWFR and solar intensity of 718W/m^2.....37

Figure 4.32 Thermal efficiency at different CWFR and solar intensity of 825W/m^2.....38

Chapter 1 Introduction

Oscillating heat pipes (OHP) have enormous benefit in thermal engineering. It has excellent ability to transport thermal heat. It needn't pumping power, its fast thermal response, simple structure, and large quantity of heat can be transported through a small cross-section area. So, it can be used in many industrial fields including solar energy water heating system. In the past time, many studies concentrated on thermal heat transfer characteristics of OHP and performance of some kinds of solar collector.

S. Rittidech and S. Wannapakne [1] investigated performance of a solar collector by closed-end oscillating heat pipes. The results confirmed that the anticipated fluctuation in efficiency of the collector depended on the time of day, solar irradiation, ambient air temperature and mean temperature of absorber plate. P. Charoensawan and P. Terdtoon [2] investigated the performance of horizontal closed-loop oscillating heat pipes (HCLOHP). They concentrated on studying the effect of tube's inner diameter, evaporator length, the number of turns, kind of working fluids, working fluid filling ratio, and operating temperature at normal operating condition. The results showed that, HCLOHP couldn't operate at lower 50^0C of evaporating section and operating temperature depended on the number of turns of the heat pipes. At evaporator temperature was equal or more than 70^0C, the CLOHP with a 2mm inner diameter started to operate at the critical number of 11 turns. The performance of the HCLOHP was improved by increasing the evaporator temperature and decreasing the evaporator length. Water and ethanol were acceptable for

working fluids. However, 30% of filling ratio was suitable for 150mm of the evaporator length. Filling ratios were both 50% and 30% for the evaporator length of 50mm. S. Rittidech, P. Terdtoon, M. Murakami, P. Kamonpet and W. Jompakdee [3] studied the effect of working fluids (R123, Ethanol), inner diameter and number of turns of closed-end oscillating heat pipes on the heat flux. R. R. Avezov, V. G. Dyskin and N. R. Avezova [4] simulated to get the optimal thermal-engineering closed air layer for a light-absorbing heat exchanger panel-transparent cover system. M. Mahasudan, G. N. Tiwari, D. S. Hrishikeshan and H. K. Sehgal [5] researched the optimization of heat loss in normal and converse flat-plate collector configurations. Heat loss was minimized by optimizing the absorber plate to glass cover separation, providing low emissivity surface on the collector's back face and spacing an additional reflector supported on glass wool insulation behind the back face. S. H. Yoon, C. Oh, and J. H. Choi [6] investigated the heat transfer characteristics of self oscillating heat pipes. The result showed that the effective thermal conductivity of this kind of heat pipes was 1000-2000 times in comparison with the conventional thermal conductivity of the copper. Besides, it was impossible to operate the heat pipes at filling ratios increasing beyond 60% due to lacking of inner space inside the heat pipes.

As conducting here, the effect of the air gap thickness, FR of working fluid and rate of cooling water on top heat loss and performance of a CLOHP flat-plate solar collector haven't been investigated experimentally.

Heat loss in flat-plate solar collectors (33-50%) occurs due to convective (22-30%), radiative loss (5-7%) from absorber surface to cover and radiative

loss (5-10%) through back surface [7]. To improve efficiency of the collector, convective and radiative heat loss must be minimized especially heat loss through the cover/top loss.

In this research, a CLOHP solar collector was constructed to study the effect of air gap thickness, and to investigate more detail the effect of FR of working fluid, flow rate of cooling water on top heat loss and performance of the collector. Experiment was conducted into two cases.

- First, to investigate the effect of the air gap thickness, it was set to 5mm, 15mm, 25mm and 35mm. Irradiation intensity of the solar simulation was adjusted to 200W/m^2, 400W/m^2, 500W/m^2, 600W/m^2, 700W/m^2, and 800W/m^2. Flow rate of cooling water was set to 0.15l/min. The results show that, the optimal air gap thickness is 15mm for most ranges of solar intensity.
- Second, to investigate the effect of FR and CWFR, the flow rates of cooling water were set to 0.15l/min, 0.30l/min and 0.45l/min, working fluid was filled with ratios of 30% to 80% of inner volume. Solar intensity was set to 545W/m^2, 645W/m^2, 718W/m^2 and 825W/m^2. The results show that the best performance of the collector is at filling ratios of 60% and 70% at solar intensities of 545W/m^2, 645W/m^2, and 718W/m^2, 825W/m^2. The collector operates more effectively at filling ratio of 80% than that of 50%. Flow rate cooling water of 0.15l/min and 0.30l/min give the collector higher performance than that of 0.45l/min.

Chapter 2 Theory analysis

The thermal heat loss to the surrounding is an important factor of a flat-plate solar collector. Heat loses from the plate through the glass cover known as top loss, through the back insulation known as bottom loss and through the edges of collector referred as edge loss. These losses take place by all mechanisms consisting of convection, conduction and radiation. All heat loss components from a flat-plate solar collector are shown in Fig. 2.1.

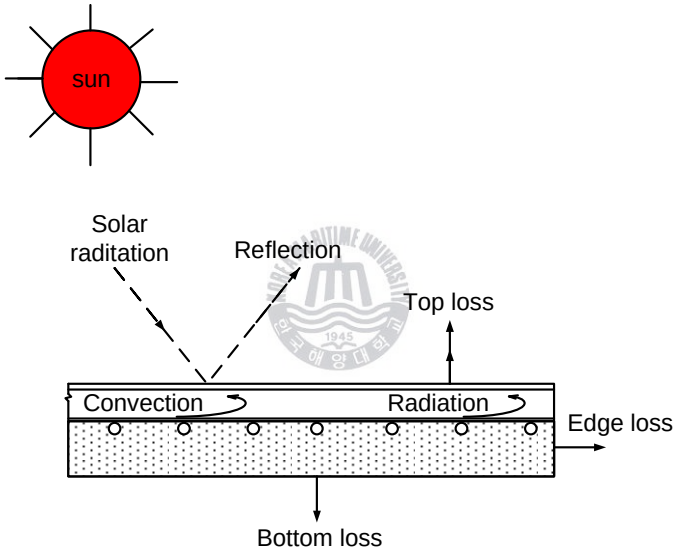

Figure 2.1 Heat losses in a flat-plate solar collector

Back and edge loss can be minimized by choosing properly insulation material and its thickness. Therefore, the most important heat loss in a flat-plate solar collector is top loss. And the factors that affect on it need to be investigated more. These steps below show some procedures to determine top heat loss of a flat-plate solar collector.

2.1 Convective heat transfer coefficient

2.1.1 Heat transfer coefficient from absorber plate to cover (h_{1c})

The convective heat transfer coefficient between absorber plate to the cover, h_{1c} , inclined an angle β to the horizontal can be calculated as [7]

$$h_{1c} = \frac{Nu.K}{L} \tag{1}$$

The Nusselt number,Nu, for air between absorber plate and glass cover is calculated as expression below [7]

$$Nu = 1 + 1.44.[a]^{+}.b + [c]^{+} \tag{2}$$

With:

$$a = 1 - \frac{1708}{Ra.cos\beta};\ b = 1 - \frac{\sin(1.8\beta)^{1.6}.1708}{Ra.cos\beta};\ c = \left\{\frac{Ra.cos\beta}{5830}\right\}^{1/3} - 1$$

The "+" exponent in formula (2) means that only the positive value of the term in square bracket is to be considered and zero is to be used for negative value, and β , the angle of inclination varies between 0^0-75^0. The Rayleigh number, Ra, is given as [7]

$$Ra = Gr.Pr = \frac{g.\beta'.\Delta T.L^3}{\nu.\alpha} \tag{3}$$

If $75° \leq \beta \leq 90°$, *Nu* is calculated as [7]

$$Nu = [1, d, e]_{max} \tag{4}$$

With:

$$d = 0.288.\left(\frac{sin\beta.Ra}{A}\right)^{1/4};\ e = 0.039.(sin\beta.Ra)^{1/3}$$

The Nusselt number, Nu, in formula (4) is the maximum value of the three quantities separated by comma and A is the ratio of length of collector plate inclined to spacing between cover and absorber plate.

2.1.2 Heat transfer coefficient from cover to ambient air (h_{2c})

The convective heat loss coefficient from cover to ambient air, h_{2c}, is given as [7]:

$$h_{2c} = 2.8 + 3V \tag{5}$$

V is the wind speed over collector in m/s.

2.2 Radiative heat transfer coefficient

2.2.1 From plate to cover (h_{1r})

The radiative heat loss coefficient from plate to cover, h_{1r}, can be given as

$$h_{1r} = \varepsilon_{ff}.\sigma.\frac{\left[(T_P + 273)^4 - (T_g + 273)^4\right]}{T_P - T_g} \tag{6}$$

With effective emissivity of plate-cover system, ε_{ff}, calculated as:

$$\varepsilon_{ff} = \left[\frac{1}{\varepsilon_P} + \frac{1}{\varepsilon_g} - 1\right]^{-1} \tag{7}$$

2.2.2 From cover to ambient (h_{2r})

Radiative heat loss coefficient from cover to ambient air, h_{2r}, can be given as

$$h_{2r} = \varepsilon_g . \sigma . \frac{\left[(T_g + 273)^4 - (T_S + 273)^4\right]}{T_g - T_a} \tag{8}$$

$$T_S = T_a - 6 \tag{9}$$

Where, $\varepsilon_g = 0.90 \div 0.94$ [8] depends on temperature of glass cover and $\varepsilon_P = 0.09$ [9].

2.3 Top loss coefficient

Total loss coefficient from plate to cover is sum of h_{1c} and h_{1r}

$$h_1 = h_{1c} + h_{1r} \tag{10}$$

And, that from the cover to ambient air

$$h_2 = h_{2c} + h_{2r} \tag{11}$$

Total top loss coefficient from plate to ambient is given as

$$U_t = \left[\frac{1}{h_1} + \frac{1}{h_2}\right]^{-1} \tag{12}$$

And, rate of top loss or total top heat loss is calculated as

$$Q_t = U_t . A_c . (T_P - T_a) \tag{13}$$

Fig. 2.2 shows a diagram of thermal circuit of a flat-plate solar collector.

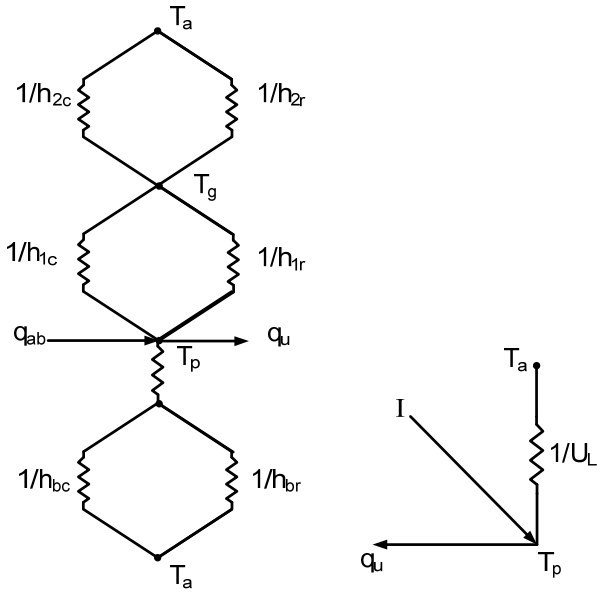

Figure 2.2 Thermal circuit diagram

To calculate top heat loss from collector, all components must be known. The formulas from (1) to (13) show that top heat loss of the collector depends on construction parameter (air gap thickness, L); environment parameters (wind velocity, V, ambient air temperature, T_a); temperatures of plate, T_P, and glass cover, T_g. Furthermore, OHP was used to transport thermal heat energy from the heating to the cooling section. Therefore, top heat loss also depends on ability of thermal heat transportation of the heat pipes. In other words, top heat loss can be affected by filling ratio of working fluid and maybe flow rate of cooling water.

Chapter 3 Collector design and experimental set-up

3.1 Collector design

The collector in this study comprises heating, adiabatic and cooling section. The oscillating heat pipes were combined with black chrome coating copper plate to absorb and transport thermal heat energy from the heating to the cooling section. Four sides and bottom of the heating section were insulated with excellent insulation material, urethane foam. The frame of the heating section was made of aluminum and transparent glass at cover. Aluminum foil was used to minimize the radiative heat loss through back surface.

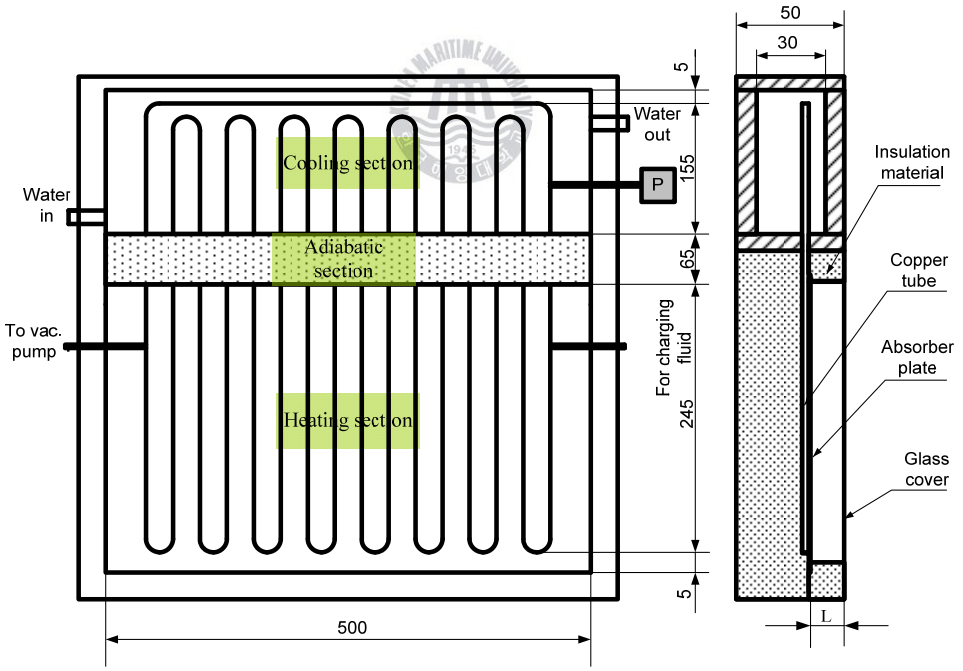

Figure 3.1 Collector dimensions and configuration

Cooling box of the collector was made of acrylic, and was wrapped around by insulation material to eliminate the effect of environment on experiments. The

detailed dimensions and photo of the collector are shown in Fig. 3.1 and Fig. 3.2.

Figure 3.2 Photo of the Collector

3.2 Experimental set-up

To determine thermal top loss from the absorber plate to ambient air, temperatures of absorber plate, glass cover and ambient air must be known. Temperatures were measured with K-type thermocouples and were recorded by MV2000-Yokogawa recorder. Cooling water for the cooling box was supplied from adjustable temperature refrigerating water bath. Its flow rate was controlled by adjusting needle valve and was observed via electrical flow meter. Schematic of experimental set-up is shown in Fig. 3.3.

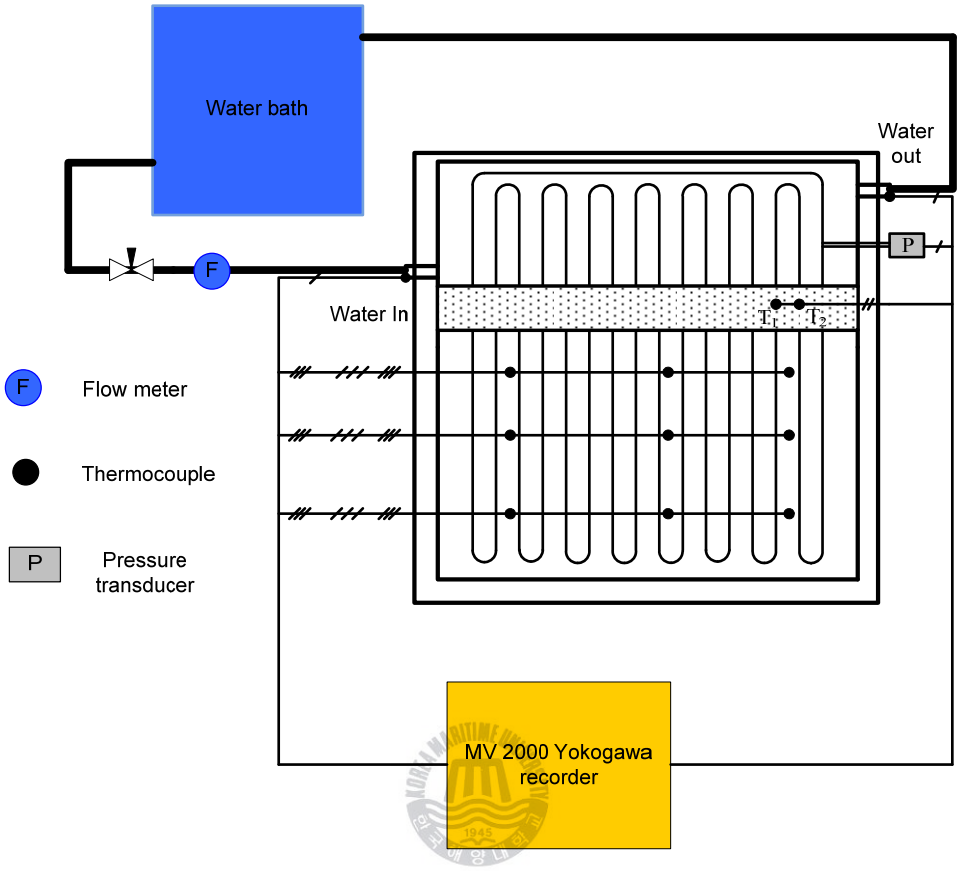

Figure 3.3 Schematic diagram of experimental set-up

Before charging working fluid into the heat pipes, air was withdrawn with vacuum-pump until pressure of 10^{-3}KPa. Pressure was checked again after one week to ensure that the vacuum couldn't be broken. During experiments, pressure inside the heat pipes was also recorded by recorder via pressure transmitter. To simulate the Solar, twelve 300W-Halogen lamps were used and attached to a flat plate that was fixed in parallel with the collector. Simulation Solar intensity was recorded with MV 2000 Yokogawa recorder via LP-PYRA-50-Pyranometer and was adjusted by adjusting transformer.

Figure 3.4 Photo of the experimental set-up

Experiment was conducted into two cases.

First, the effect of the thickness of air gap between absorber plate and glass cover on top heat loss was investigated. Solar irradiation intensity was adjusted to 200W/m^2, 400W/m^2, 500W/m^2, 600W/m^2, 700W/m^2, and 800W/m^2. The air gap thickness was set to 5mm, 15mm, 25mm and 35mm. Temperatures of absorber plate, glass cover and ambient air were recorded and then determined by averaging. Top loss coefficient and rate of top heat loss was calculated basing on recorded temperatures as shown in chapter 2.

Second, the effect of filling ratio of working fluid and flow rate of cooling water on top heat loss and performance of the collector were investigated. Heat pipes were filled with working fluid of filling ratios of 30% to 80% with 10%

increasing interval. Flow rate of water cooling was set to 0.15l/min, 0.30l/min and 0.45l/min. Irradiation intensity of the solar simulator was set to 545W/m^2, 645W/m^2, 718W/m^2, and 825W/m^2. Rate of top loss was determined to judge the effect of filling ratio of working fluid and flow rate of cooling water on performance of the collector.

Experiments were performed in Laboratory. Therefore, it could be considered no effect of wind on experiments. Temperatures of all components and pressure inside the heat pipes were recorded and were determined in period of steady condition.

Chapter 4 Results of experiment and discussions

Before surveying the effect of some parameters on top heat loss, some assumptions are given:

- Emissivity of absorber plate and glass cover is constant in ranges of temperature;
- Simulation solar intensity is constant at each step;
- The effects of light and environmental conditions on the cooling box of the collector is negligible;
- Wind velocity is considered to be zero.

4.1 Effect of the air gap thickness on thermal top heat loss

Temperatures and pressure inside the heat pipes of the collector were measured and recorded simultaneously during experiments. Temperatures of absorber plate, glass cover were determined by averaging recorded values. Thermocouples were attached to two adjacent copper tubes in the adiabatic section to check whether the copper tubes worked as oscillating heat pipes or not. If temperatures at these points always change alternately, this means that temperature of one tube is sometimes higher than the others and vice versa, the copper tubes will work as oscillating heat pipes. If this phenomenon does not happen or temperature of one copper tube is always higher than the others or vice versa, it also means that working fluid inside the heat pipes does not circulate and thus the collector does not work effectively.

The change of temperature of absorber plate is shown in Fig. 4.1.

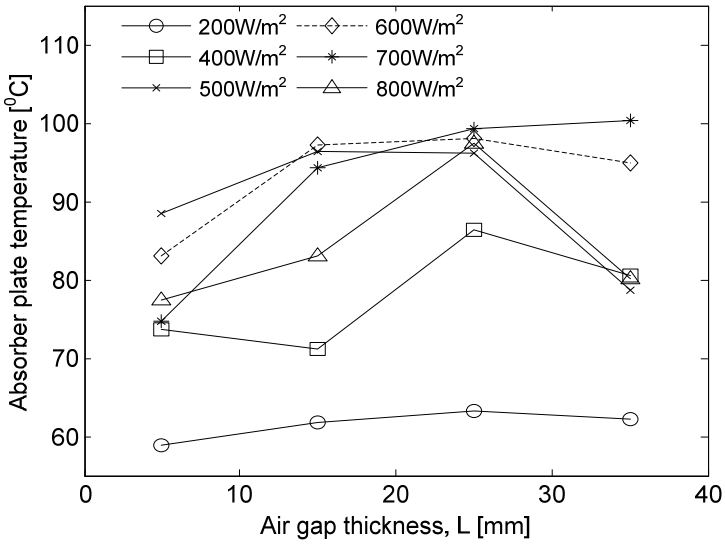

Figure 4.1 Absorber plate temperature vs. air gap thickness

It shows that, temperature of absorber plate depends strongly on the air gap thickness of the collector. At first, temperature of absorber plate increases with increasing of the air gap thickness. It decreases with increasing of the air gap thickness beyond 25mm. Temperature of absorber plate at 800W/m^2 of solar intensity is smaller than that at 500W/m^2, 600W/m^2, and 700W/m^2. Since, it is high enough energy to supply for evaporating working fluid inside the heat pipes and it makes the working fluid oscillate quickly. Therefore, thermal heat can be transported more perfectly from the heating to the cooling section.

Temperature of glass cover and difference temperature of absorber plate and glass cover are shown in Fig. 4.2 and Fig. 4.3.

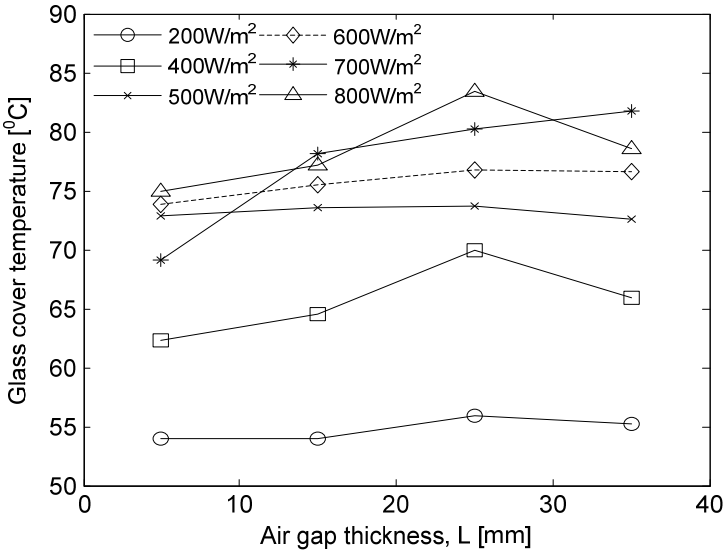

Figure 4.2 Glass cover temperature vs. air gap thickness

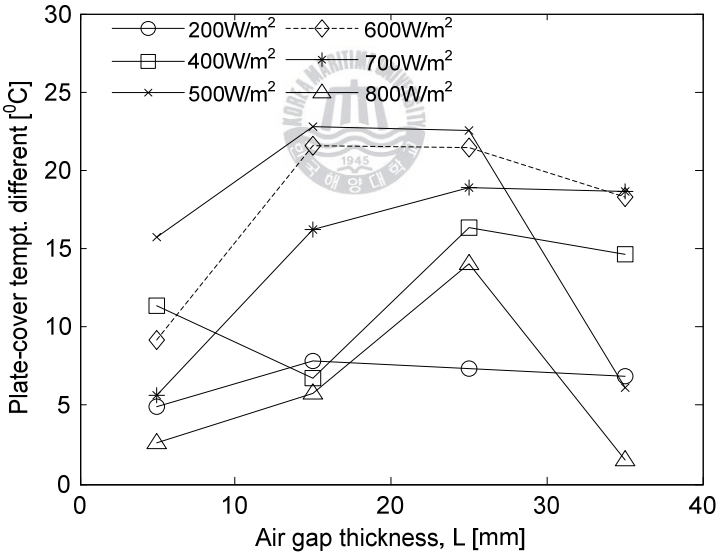

Figure 4.3 Plate - cover temperature difference vs. air gap thickness

Fig. 4.2 shows that, temperature of cover depends not very strongly on the air gap thickness of the collector. It is almost high at the air gap thickness of 25mm.

Effect of the air gap thickness on convection heat transfer coefficient from absorber plate to glass cover is shown in Fig. 4.4. Convective heat transfer coefficient reaches to maximum at the air gap thickness of 5mm and minimum at 15mm in most ranges of the solar irradiation intensity.

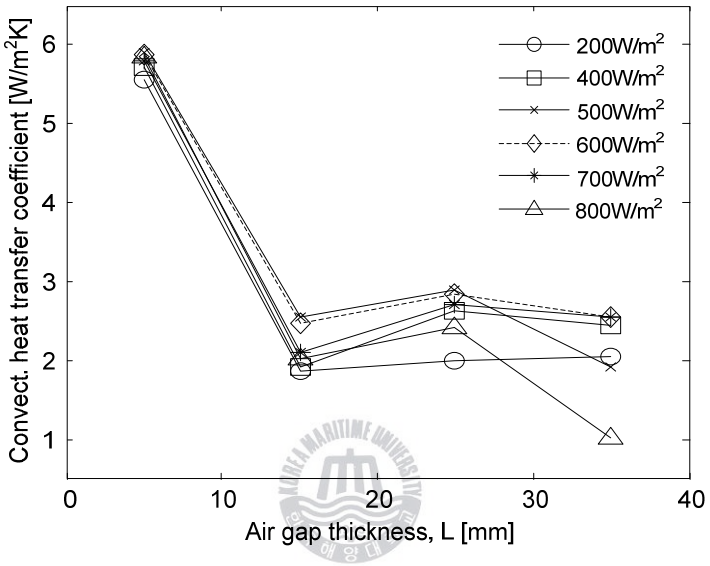

Figure 4.4 Convective heat transfer coefficient vs. air gap thickness

Because at the air gap thickness of 5mm, heat conduction happen very intensively. At this air gap thickness, convective heat transfer coefficient is equal to conduction heat transfer coefficient due to the Nusselt number is equal to unity in this case. Therefore, convective heat transfer coefficient is very high at 5mm of the air gap thickness. The convective heat transfer coefficient at irradiation intensity of 800W/m^2 is small because it is enough energy for the heat pipes working effectively. At the air gap thickness of 15mm, the Nusselt number is little bigger than unity, but at this thickness it is enough to make high thermal conduction resistance that makes low heat loss coefficient. Therefore, total top loss coefficient is minimized at the air gap thickness of 15mm as shown in Fig. 4.5.

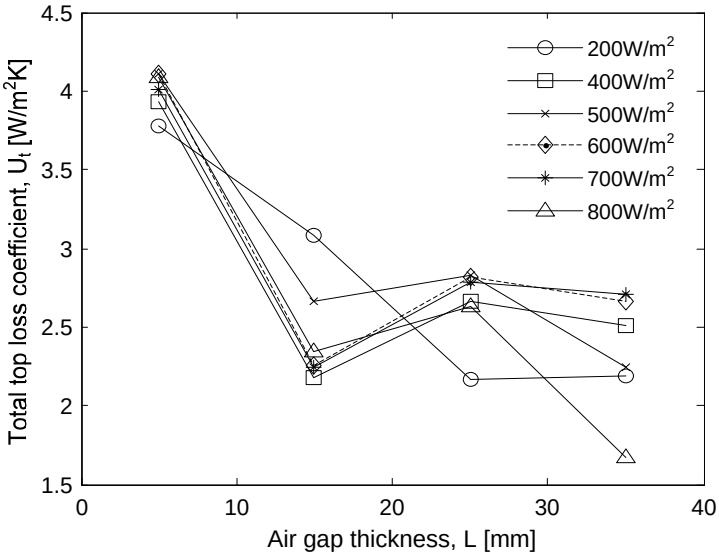

Figure 4.5 Total top loss coefficient vs. air gap thickness

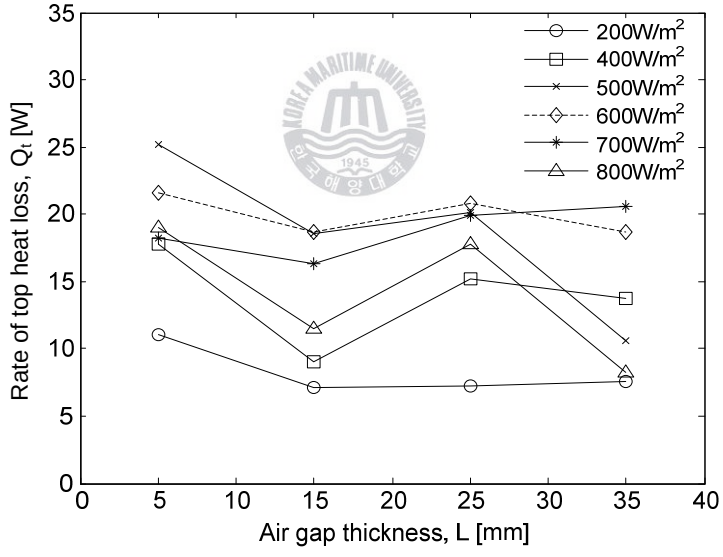

Figure 4.6 Rate of top heat loss vs. air gap thickness

The change of rate of top heat loss is similar to the change of total top loss coefficient and is shown in Fig. 4.6. It can be seen that rate of top heat loss is minimum at the air gap thickness of 15mm in almost ranges of solar irradiation

intensity. Because the convective heat-transfer coefficient and total top loss coefficient is minimum at 15mm of the air gap thickness.

Effect of the air gap thickness on the performance of collector can be judged by the ratio of rate of top loss to incident solar energy. The change of this ratio versus the air gap thickness in wide ranges of solar irradiation intensity is shown in Fig. 4.7.

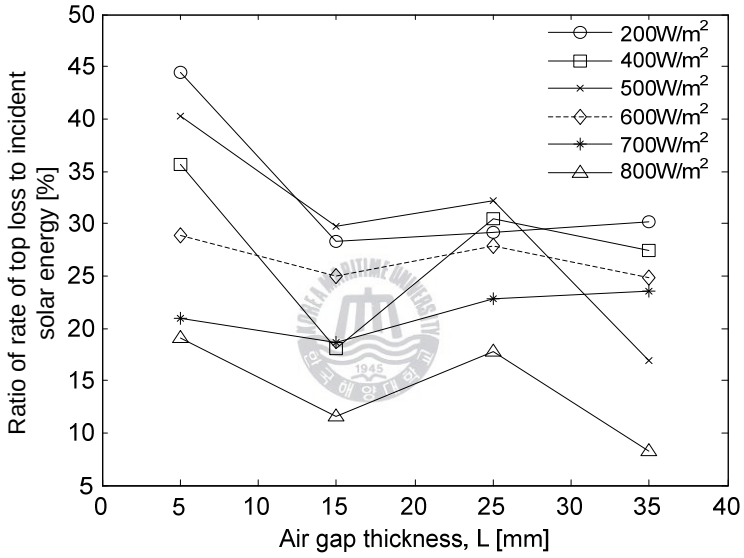

Figure 4.7 Ratio of top loss to incident solar energy vs. air gap thickness

In all ranges of irradiation intensity, this ratio has tendency to decrease, increase and then decrease in later case of the air gap thickness. Because of the change of rate of top loss at different air gap thickness is shown in Fig. 4.6. The higher the solar irradiation intensity is, the smaller the ratio of top loss to incident solar irradiation is. Since, at high solar intensity, the collector operates more effectively due to the heat pipes work more perfectly. Therefore, much more thermal heat can be transported from the heating to the cooling section of

the collector. At low solar irradiation intensity, working fluid circulates not very quickly, thus more thermal heat energy can be stagnated inside the heating section and much more heat is lost. Fig. 4.7 shows that the smallest ratio of rate of top loss to incident solar energy, which gives the highest efficiency for the collector, is at the air gap thickness of 15mm for most ranges of solar radiation intensity.

4.2 Effect of FR on top loss and thermal performance of the collector

Temperatures of absorber plate and cover are shown in Fig. 4.8 and Fig. 4. 9.

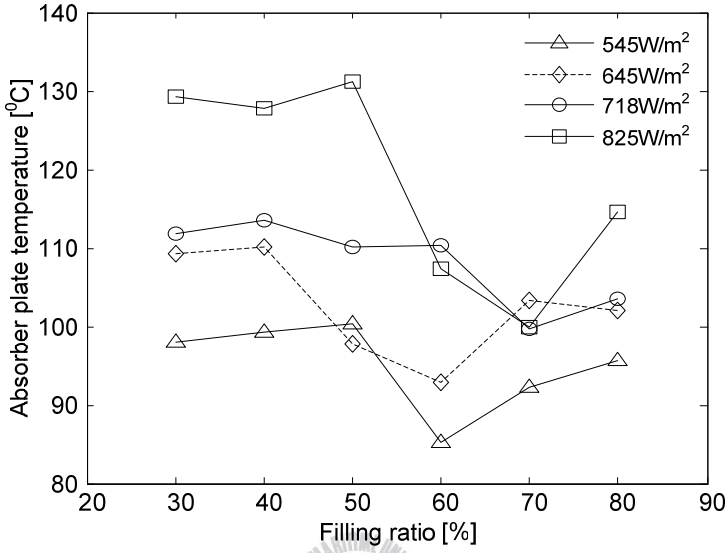

Figure 4.8 Absorber plate temperature vs. filling ratio

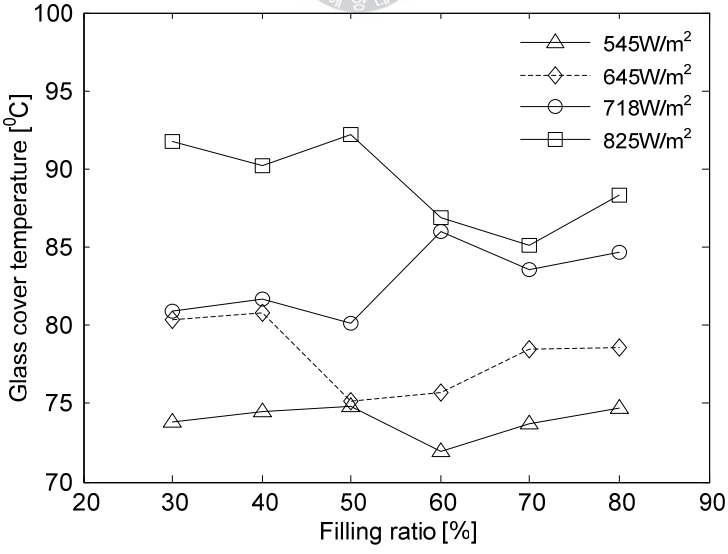

Figure 4.9 Glass cover temperature vs. filling ratio

Fig. 4.8 shows that temperature of absorber plate depends strongly on filling ratio of working fluid. Fig. 4.9 shows that the change of temperature of glass cover versus FR is not as much as the change of temperature of absorber plate.

First, temperature of the absorber plate almost remains constant at filling ratios of 30%, 40% and 50%. It decreases dramatically at FR of 60% and 70% at solar irradiation intensities of 545W/m^2, 645W/m^2 and 718W/m^2, 825W/m^2. Furthermore, temperature of the absorber plate increases with increasing of filling ratios beyond 70%. Since, at filling ratios of 30% and 40%, it is not enough working fluid inside the heat pipes to create alternately liquid slugs and vapor bubbles which transport thermal heat energy from the heating to the cooling section. In other words, dry-out phenomenon happens inside the heat pipes at filling ratios of 30% and 40%. If dry-out phenomenon happens, this means that there is no alternately formation of vapor bubbles and liquid slugs inside the heat pipes. Therefore temperatures at two points of two adjacent copper tubes cannot increase and decrease alternately. Besides, without formation of liquid slugs and vapor bubbles, pressure inside the heat pipes almost remains constant. Temperatures at two points on the copper tubes are shown as T_1 and T_2 and pressure inside the heat pipes is shown as P in Fig. 4.10 - Fig. 4.15 and Fig. 4.17 – Fig. 4.25. Figures 4.10 and Fig. 4.1 show that the dry-out phenomenon happens at filling ratios of 30% and 40%. Since, the length of the heating section of the heat pipes in this study is longer than that in some previous studies. Therefore, it needs more working fluid to create alternately vapor bubbles and liquid slugs or it needs more working fluid to avoid the dry-out phenomenon happening inside the heat pipes.

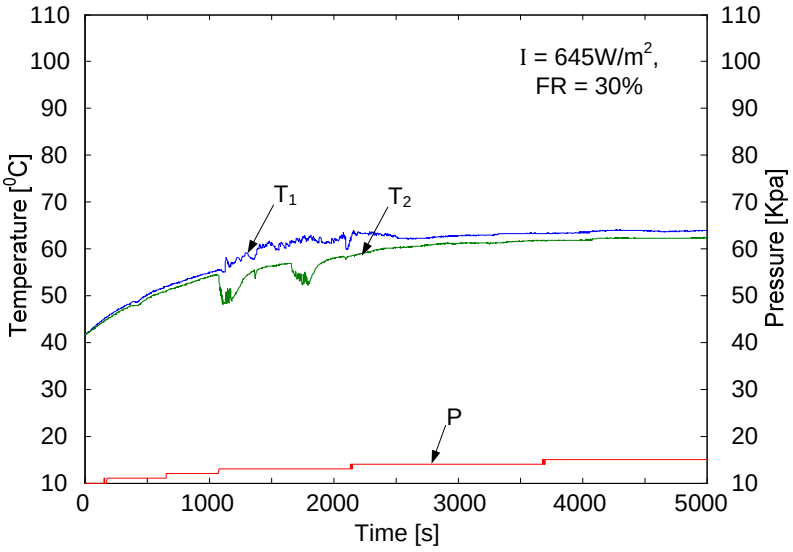

Figure 4.10 **T_1, T_2, P** ***vs. time at filling ratio of 30% and solar intensity of 645W/m^2***

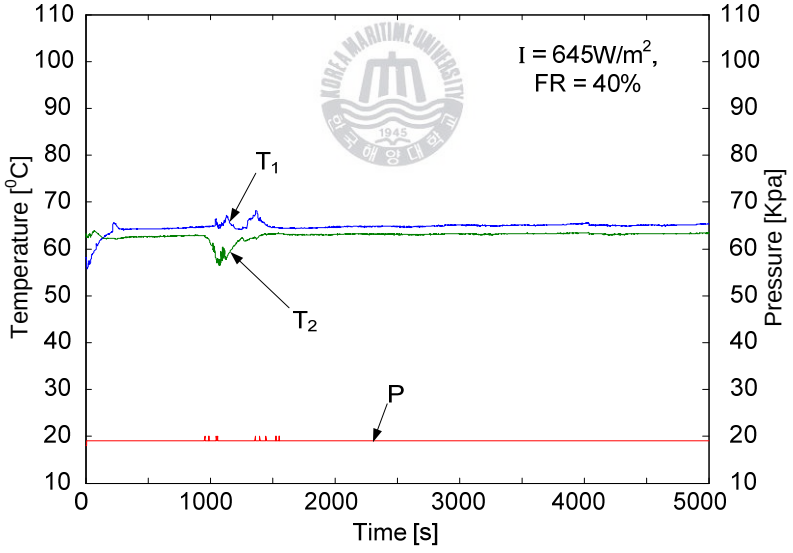

Figure 4.11 **T_1, T_2, P** ***vs. time at filling ratio of 40% and solar intensity of 645W/m^2***

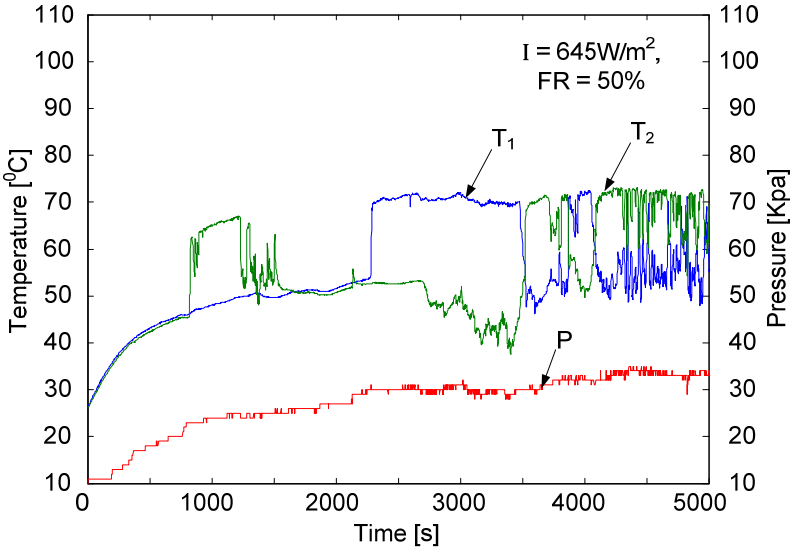

Figure 4.12* T_1, T_2, P *vs. time at filling ratio of 50% and solar intensity of 645W/m^2

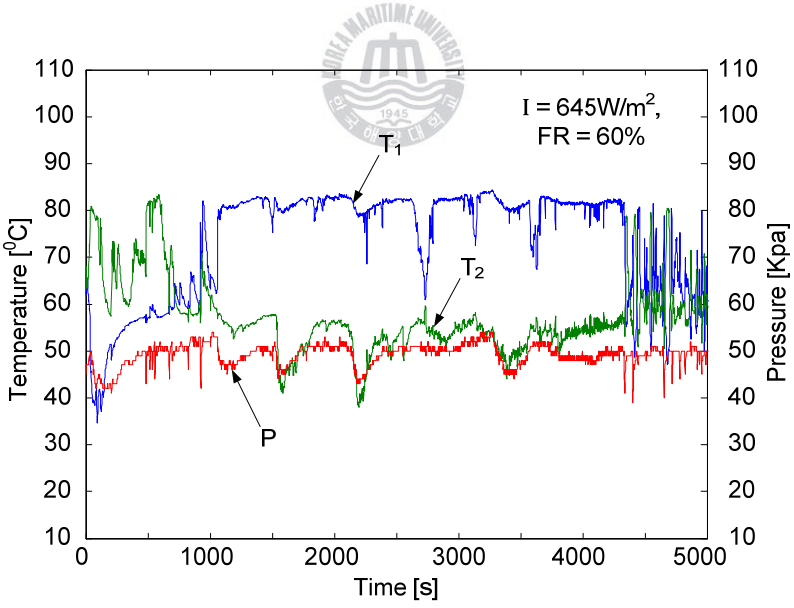

Figure 4.13* T_1, T_2, P *vs. time at filling ratio of 60% and solar intensity of 645W/m^2

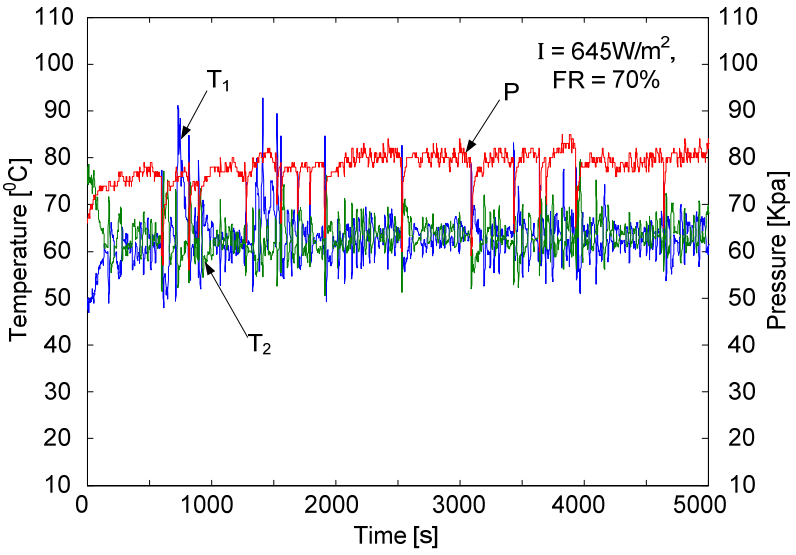

Figure 4.14 **T_1, T_2, P** ***vs. time at filling ratio of 70% and solar intensity of 645W/m^2***

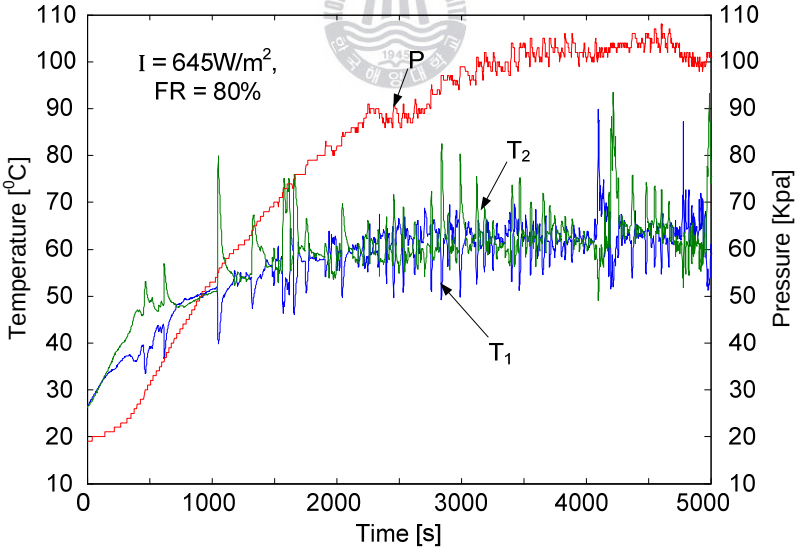

Figure 4.15 **T_1, T_2, P** ***vs. time at filling ratio of 80% and solar intensity of 645 W/m^2***

Fig. 410 – Fig. 4.15 show that the collector works more intensively at filling ratios of 60%, 70% and 80% than that at FR of 50%. Since, it is enough working fluid to create vapor bubbles and liquid slugs alternately at filling ratios of 60% and 70%. Thus temperatures, T_1, T_2 and pressure, P, change more quickly, the magnitude of its change is also bigger at FR of 60% and 70%. This makes the heat pipes work more intensively thus the collector works more effectively. This is also the reason why it makes temperature of the absorber plate different at different filling ratio as shown in Fig. 4.8.

Total top loss coefficient of the collector versus filling ratio of working fluid is shown in Fig. 4.16.

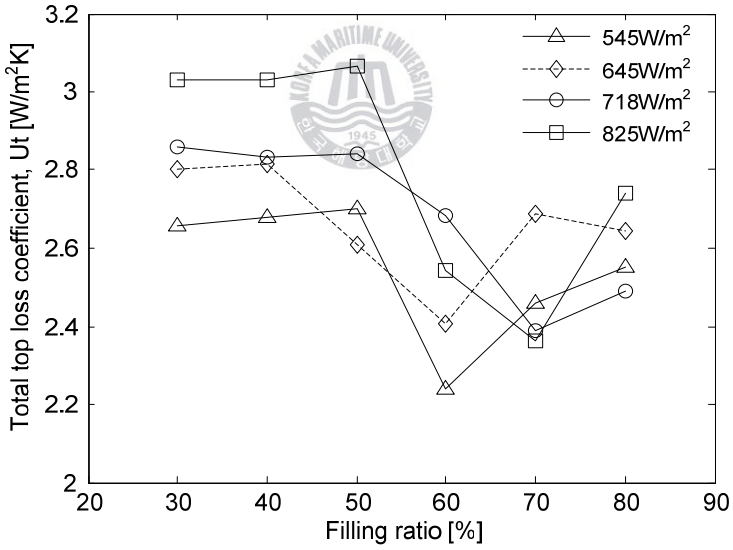

Figure 4.16 Total top loss coefficient vs. filling ratio

It shows that top loss coefficient of the collector depends intensively on filling ratio of working fluid. Top loss coefficient is almost the same at filling ratios of 30% and 40%. Because at these filling ratios, the dry-out phenomenon

happens that makes the temperature of absorber plate very high thus the high of total top loss coefficient.

Total top loss coefficient decreases dramatically at filling ratio of 60% and solar irradiation intensities of 545W/m^2 and 645W/m^2. At solar irradiation intensities of 718W/m^2 and 825W/m^2, it decreases dramatically at FR of 70%. Since, 60% and 70% of filling ratios are suitable for the heat pipes working intensively as explained before. The change of T_1, T_2 and P at FR of 30%, 40% and 50% at solar intensities of 545W/m^2, 718W/m^2 and 825W/m^2 are similar to the case of its at solar intensity of 645W/m^2 (Fig. 4.10 and Fig. 4.11 and Fig. 4.12). It means that the dry-out phenomenon happens at FR of 30%, 40% and the collector cannot work perfectly at FR of 50%. The change of T_1, T_2 and P versus time at filling ratios of 60%, 70%, 80% and solar intensities of 545W/m^2, 718W/m^2, and 825Wm^2 are shown in Fig. 4.17 - Fig. 4.25 as below. It indicates that the heat pipes work smoothly and more stably at FR of 60%, 70% and 80%, especially at FR of 60% and 70%. Since, temperatures, T_1, T_2 and pressure, P changes intensively at FR of 60% and 70%. Therefore the collector works more perfectly at FR of 60% and 70%.

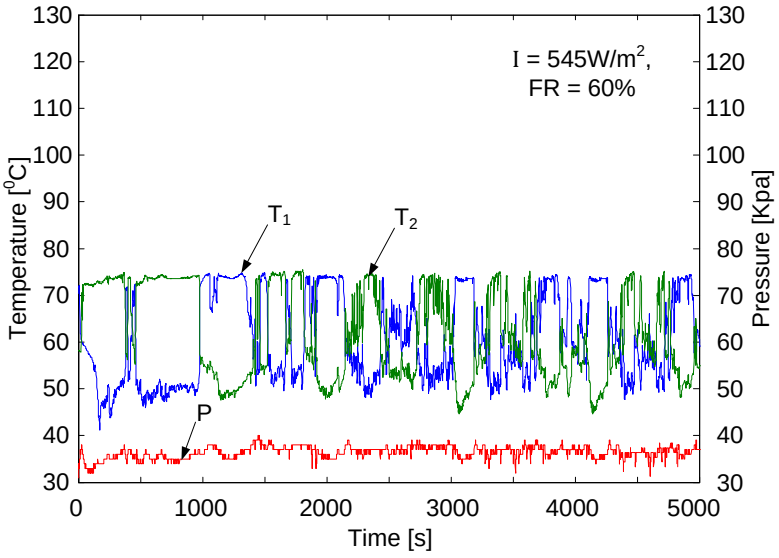

Figure 4.17 **T_1, T_2, P** ***vs. time at filling ratio of 60% and solar intensity of 545W/m^2***

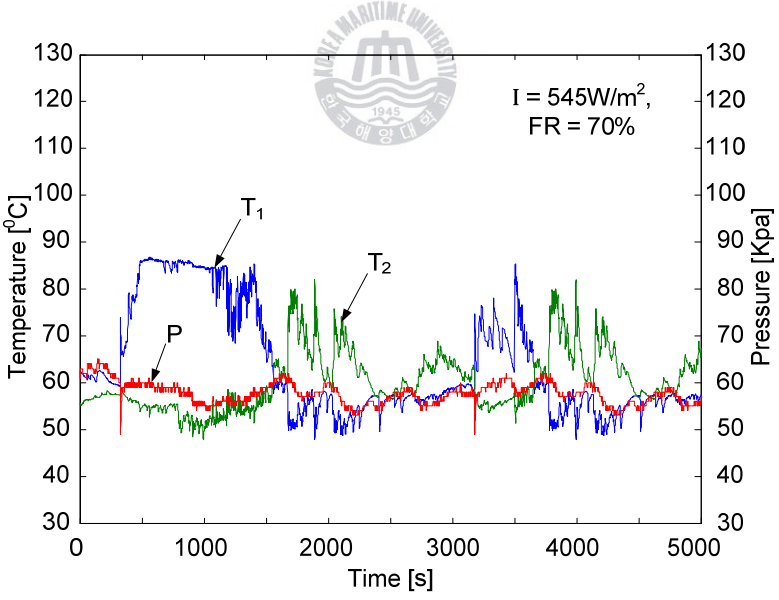

Figure 4.18 **T_1, T_2, P** ***vs. time at filling ratio of 70% and solar intensity of 545W/m^2***

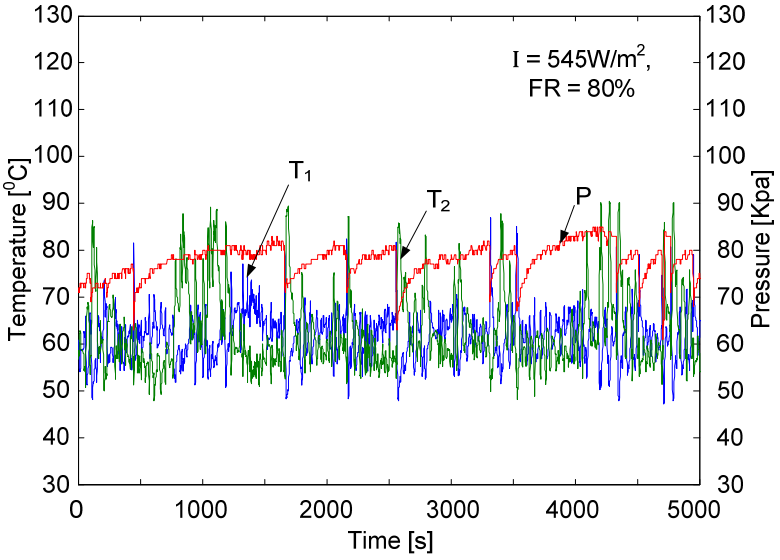

Figure 4.19* T_1, T_2, P *vs. time at filling ratio of 80% and solar intensity of 545W/m^2

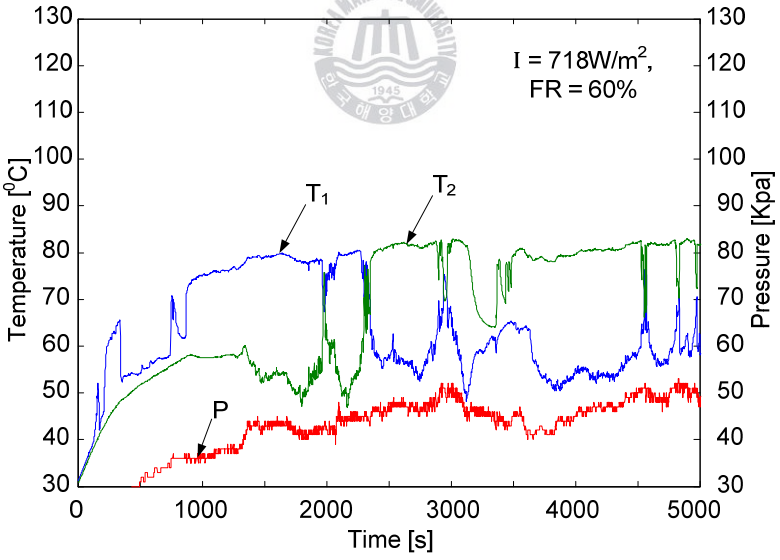

Figure 4.20* T_1, T_2, P *vs. time at filling ratio of 60% and solar intensity of 718W/m^2

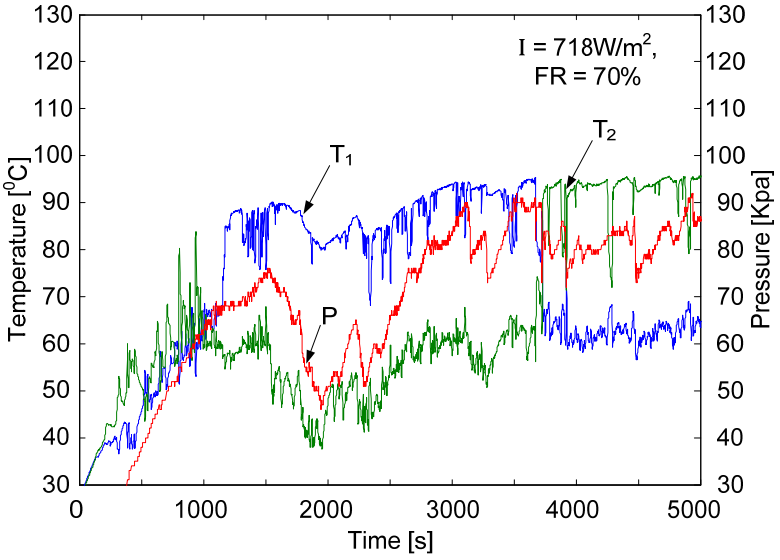

Figure 4.21 **T_1, T_2, P** ***vs. time at filling ratio of 70% and solar intensity of 718W/m^2***

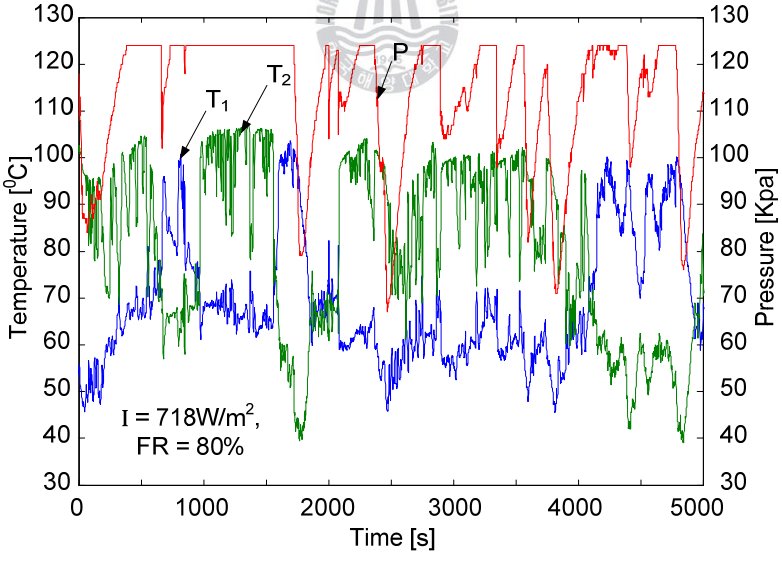

Figure 4.22 **T_1, T_2, P** ***vs. time at filling ratio of 80% and solar intensity of 718W/m^2***

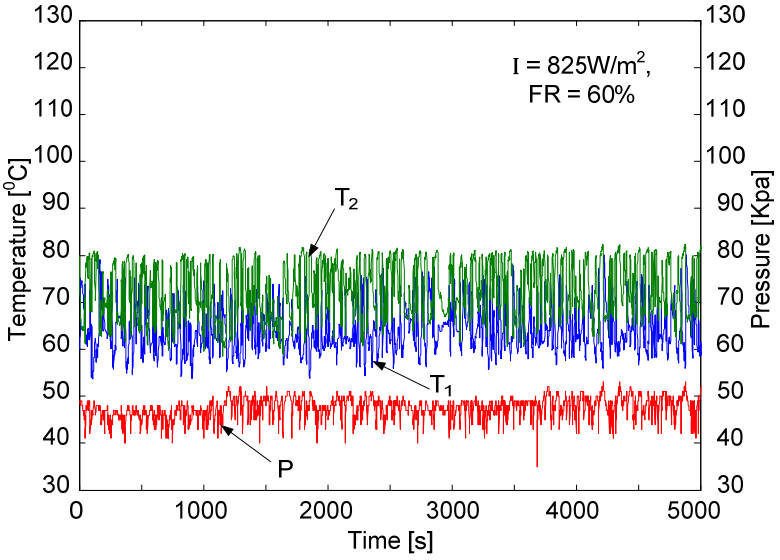

Figure 4.23 **T_1, T_2, P** ***vs. time at filling ratio of 60% and solar intensity of 825W/m^2***

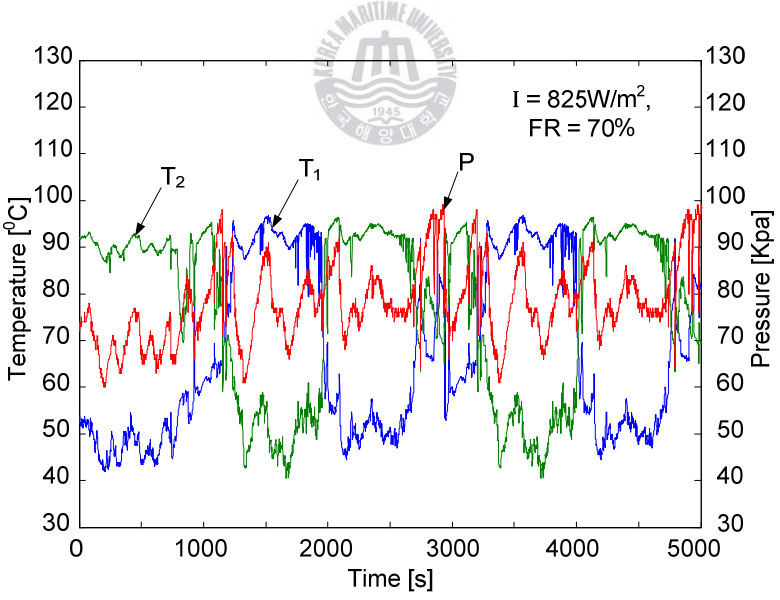

Figure 4.24 **T_1, T_2, P** ***vs. time at filling ratio of 70% and solar intensity of 825W/m^2***

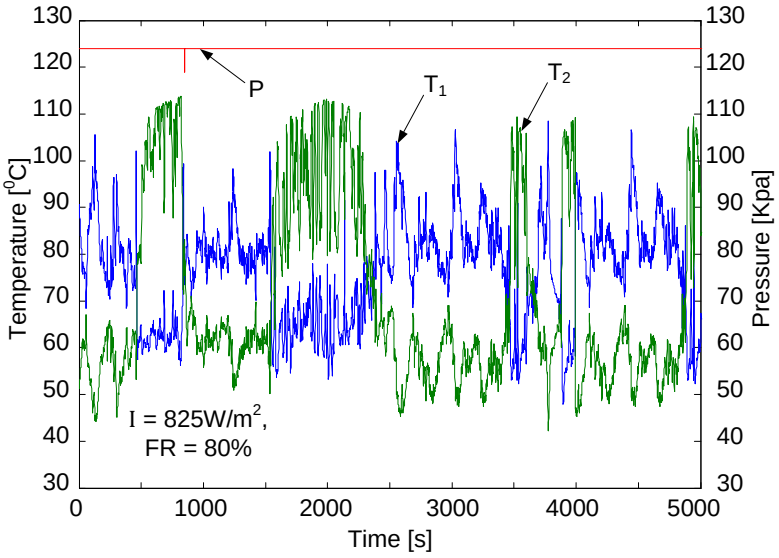

Figure 4.25* T_1, T_2, P *vs. time at filling ratio of 80% and solar intensity of 825W/m^2

Rate of top heat loss, Q_t is determined via top heat loss coefficient as shown in chapter 2. Rate of top heat loss versus filling ratio is shown in Fig. 4.26. Like the top loss coefficient, rate of top heat loss reaches to minimum at FR of 60%, and 70% and solar irradiation intensities of 545W/m^2, 645W/m^2 and 718W/m^2, 825W/m^2, respectively. At FR of 30%, 40% and 50%, it is not enough working fluid for the heat pipes working perfectly to transport thermal heat energy to the cooling section. Therefore thermal heat is stagnated in the heating section that leads on high of the rate of top heat loss.

Effect of filling ratio on performance of the collector can be estimated by the ratio of rate of top loss to incident solar energy. This ratio is shown in the Fig. 4.27.

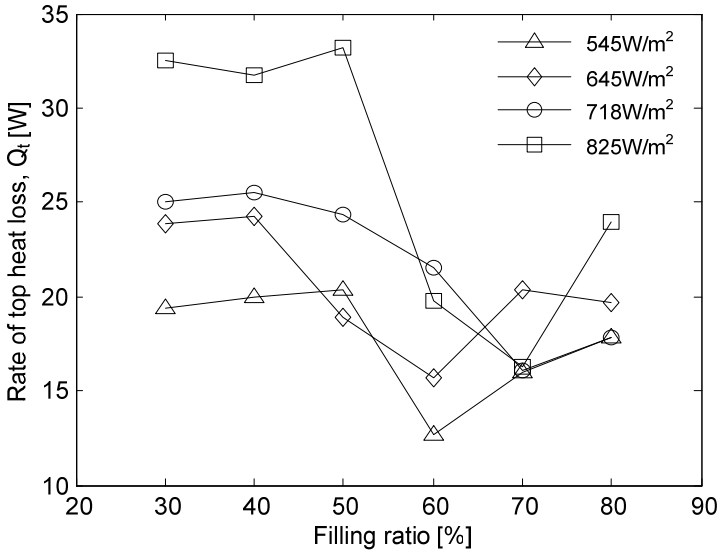

Figure 4.26 Rate of top heat loss vs. filling ratio

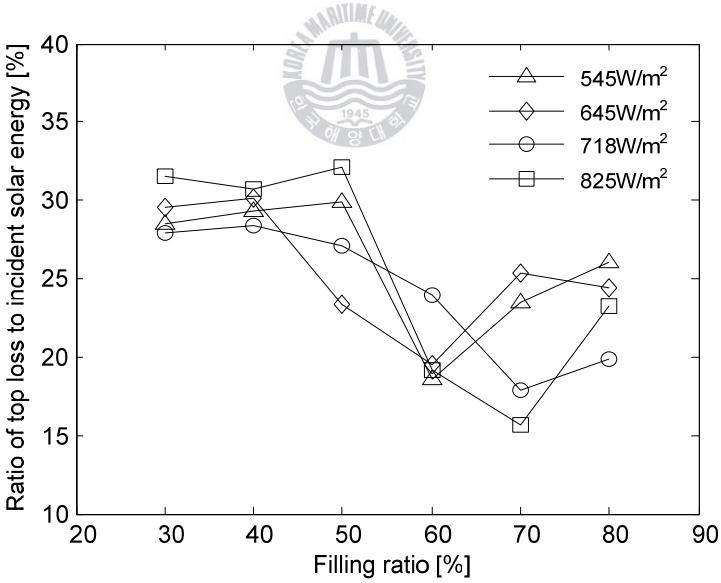

Figure 4.27 Ratio of top loss to incident solar energy vs. filling ratio

Fig. 4.27 shows that filling ratio of working fluid has dominant effect on thermal performance of the collector. The higher the ratio of rate of top loss to incident solar energy is, the smaller the collector's thermal performance is. Thermal performance of the collector depends on not only filling ratio but also solar irradiation intensity. Because at solar intensities of 545W/m^2 and 645W/m^2, filling ratio of working fluid of 60% is enough to create alternately vapor bubbles and liquid slugs inside the heat pipes. But, at solar intensities of 718W/m^2 and 825W/m^2, working fluid inside the heat pipes vaporizes more quickly thus it needs more working fluid. Therefore filling ratio of 70% is suitable for solar intensities of 718W/m^2 and 825W/m^2. However, at filling ratios increasing beyond 80%, it's not enough vacuum space for creating intensively vapor bubbles. In this circumstance, the less vapor bubbles can be created inside the heat pipes. Therefore, pressure wave along the heat pipes cannot be created intensively. This reduces ability of thermal transportation of the heat pipes. However, the ratio of rate of top loss to incident solar energy at filling ratio of 80% is almost smaller than that at FR of 50% as shown in Fig. 4.27. It indicates that the collector operates more effectively at FR of 80% than that of 50%.

Thermal efficiency of the collector can be determined as expression:

$$\eta = \frac{q_u}{I.A_c} = \frac{m.C.\Delta T_{cw}}{I.A_c}$$

Thermal efficiency of the collector versus filling ratio at different solar intensity is shown in Fig. 4.28. As analyzing above, rate of top loss has dominant effect on the performance of the collector.

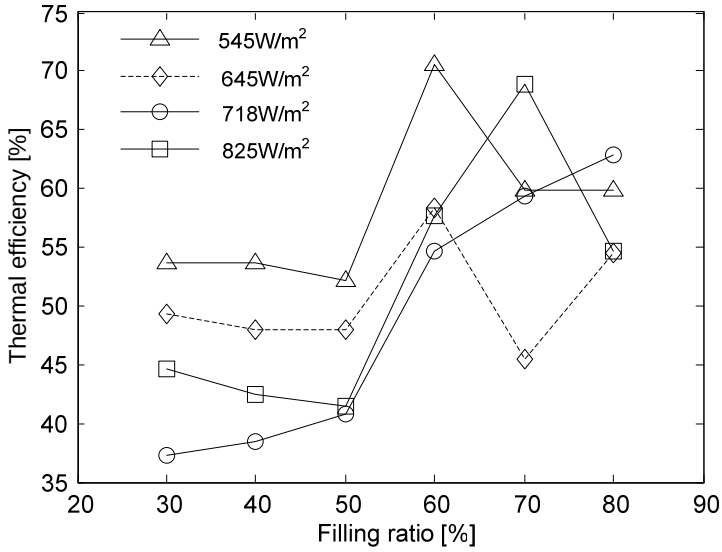

Figure 4.28 Thermal efficiency vs. filling ratio at different solar intensity

The filling ratios that make high of top heat loss make low thermal efficiency and vice versa. Thermal efficiency reaches to maximum at filling ratios of 60% and 70% at 545W/m^2, 645W/m^2 and 718W/m^2, 825W/m^2. This is because the rate of top loss of the collector reaches to minimum at FR of 60% and 70% in these ranges of solar intensity. Therefore the optimal filling ratio of working fluid for the heat pipes of this collector is 60% and 70% for different range of solar irradiation intensity.

4.3 Effect of flow rate of cooling water on the thermal performance of the collector

The effect of the cooling water flow rate on the thermal efficiency of the collector is shown in figures 4.29 - 4.32.

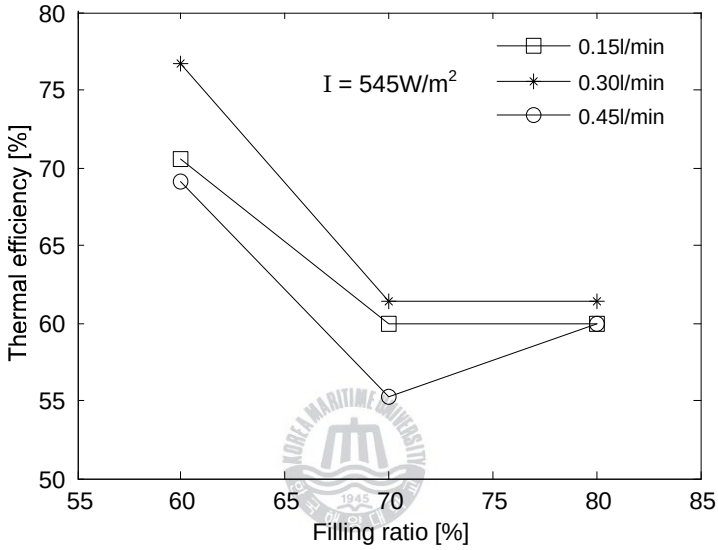

Figure 4.29 Thermal efficiency at different CWFR and solar intensity of 545W/m^2

It can be seen that thermal efficiency of the collector is almost higher at flow rates of cooling water of 0.15l/min and 0.30l/min than that at flow rate of 0.45l/min. Fig. 4.30 shows that, thermal efficiency at flow rate of 0.45l/min is just a little higher or even though is equal to that at flow rate of 0.30l/min at FR of 80%. This is because at bigger rate of flow, the bubbles inside the cooling section of the heat pipes can be collapsed so quickly that makes unbalance between vapor bubbles and liquid slugs. And, in the oscillating heat pipes, thermal can be transported mainly by sensible heat of the liquid slugs.

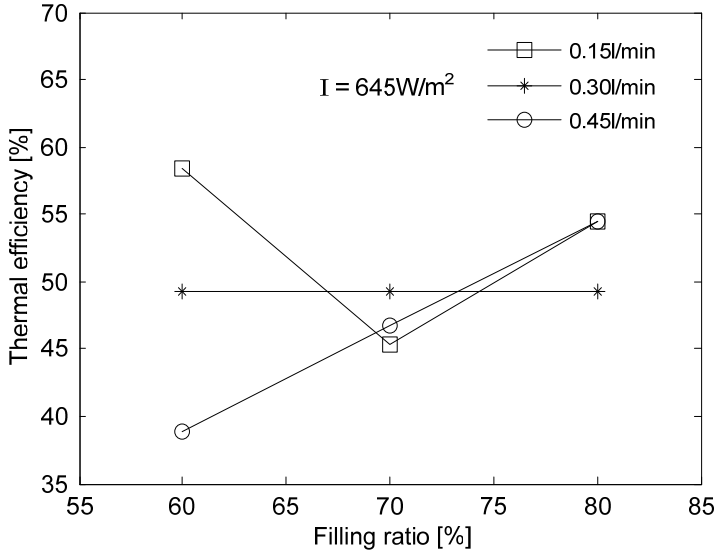

Figure 4.30 Thermal efficiency at different CWFR and solar intensity of 645W/m^2

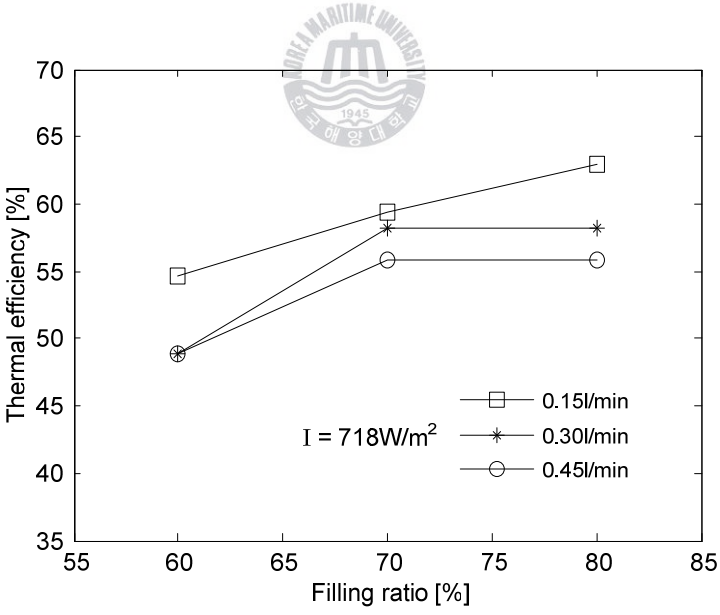

Figure 4.31 Thermal efficiency at different CWFR and solar intensity of 718W/m^2

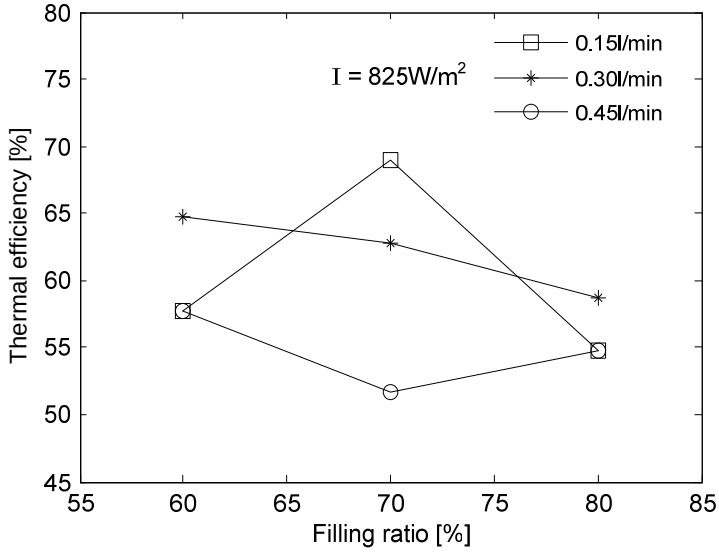

Figure 4.32 Thermal efficiency at different CWFR and solar intensity of 825W/m^2

Vapor bubbles have function of making pressure wave to transport liquid slugs from the heating to the cooling section of the heat pipes. At high flow rate of cooling water, it is lack of vapor bubbles making pressure wave due to the bubbles is collapsed so quickly. Thus it makes low ability of thermal heat energy transportation of the heat pipes. Therefore it makes low thermal efficiency of the collector at high flow rate of cooling water.

Chapter 5 Conclusions

In this research, experiments on a closed-loop oscillating heat pipes flat-plate solar collector were performed to investigate the effect of air gap thickness between absorber plate and glass cover, filling ratio of working fluid, and flow rate of cooling water on top heat loss and performance of the collector.

Thermal top loss coefficient and top loss of the collector depend on both the air gap thickness and solar irradiation intensity. The optimal air gap thickness of the collector is 15mm for most ranges of solar intensity. At this air gap thickness, the collector can give the highest performance due to the smallest of the top loss.

The best performance of the collector can be reached at filling ratios of working fluid of 60%, 70% at solar irradiation intensities of 545W/m^2, 645W/m^2, and 718W/m^2, 825W/m^2, respectively. Dry-out phenomenon happens at filling ratios of 30% and 40%. The collector operates more effectively at filling ratio of 80% than that at FR of 50%.

Cooling water flow rates at 0.15l/min and 0.30l/min give the collector better performance than that at flow rate of 0.45l/min.

References

[1] S. Rittidech, S. Wannapakne, *Experiment study of the performance of a solar collector by closed-end oscillating heat pipe*, Applied thermal engineering 27, pp 1978-1985, 2007.

[2] P. Charaensawan, P. Terdtoon, *Thermal performance of horizontal closed-loop oscillating heat pipes*, Applied thermal engineering 28, pp 460-466, 2008.

[3] S. Rittidech, P. Terdtoon, M. Murakami, P. Kamonpet, W. Jompakdee, *Correlation to predict heat transfer characteristics of a closed-end oscillating heat pipe at normal operating condition*, Applied thermal engineering 23, pp 495-510, 2003.

[4] R. R. Avezov, V. G. Dyskin, N. R. Avezova, *Thermal optimization of closed air layer of a light-absorbing heat exchange panel-transparent cover system of water-heating flat-plate solar collectors*, ISSN 0003-701X, Applied solar energy, vol. 43, No. 4, pp 207-210, 2007.

[5] M. Mahasudan, G. N. Tiwari, D. S. Hrishikeshan and H. K. Sehgal, *Optimization of heat losses in normal and reverse flat-plate collector configurations: Analysis and performance*, Energy con.& Mgmt vol. 21, pp 191-198, 1981.

[6] S. H. Yoon, C. Oh, and J. H. Choi, *A study on the Heat transfer characteristics of self-oscillating heat pipe*, KSME international Journal, Vol. No. 3, pp 354-362, 2002.

[7] G.N. Tiwari, *Solar energy fundamental, design, modeling and application*, Center for Energy study, Indian Institute of Technology, Delhi, New Delhi-110 016, India, 2002.

[8] K. Ražnjević, *Handbook of Thermodynamic tables and charts*. Semisphere publishing corperation, 1976.

[9] Y. A. çengel, *Heat transfer*, 2nd edition, Mc Graw Hill, 2003.